

Renormalization analysis of intermittency in two coupled maps

Sang-Yoon Kim

Department of Physics

Kangwon National University

Chunchon, Kangwon-Do 200-701, Korea

Abstract

The critical behavior for intermittency is studied in two coupled one-dimensional (1D) maps. We find two fixed maps of an approximate renormalization operator in the space of coupled maps. Each fixed map has a common relevant eigenvalue associated with the scaling of the control parameter of the uncoupled one-dimensional map. However, the relevant “coupling eigenvalue” associated with coupling perturbation varies depending on the fixed maps. These renormalization results are also confirmed for a linearly-coupled case.

PACS numbers : 05.45.+b, 03.20.+i, 05.70.Jk

Keywords: Renormalization, Intermittency, Coupled Maps

arXiv:chao-dyn/9807036v1 27 Jul 1998

A route to chaos via intermittency in the one-dimensional (1D) map is associated with a saddle-node bifurcation [1]. Intermittency just preceding a saddle-node bifurcation to a periodic attractor is characterized by the occurrence of intermittent alternations between regular behavior and chaotic behavior. Scaling relations for the average duration of regular behavior in the presence of noise have been first established [2] by considering a Langevin equation describing the map near the intermittency threshold and using Fokker-Plank techniques. The same scaling results for intermittency have been later found [3] by employing the same renormalization-group equation [4] for period doubling with a mere change of boundary conditions appropriate to a saddle-node bifurcation.

Recently, universal scaling results of period doubling for the 1D map have been generalized to the coupled 1D maps [5–9], which are used to simulate spatially extended systems with effectively many degrees of freedom [10]. It has been found that the critical scaling behaviors of period doubling for the coupled 1D maps are much richer than those for the uncoupled 1D map [8,9]. These results for the abstract system of the coupled 1D maps are also confirmed in the real system of the coupled oscillators [11]. Similarly, the scaling results of the higher period p -tuplings ($p = 3, 4, \dots$) in the 1D map are also generalized to the coupled 1D maps [12]. Here we are interested in another route to chaos via intermittency in coupled 1D maps. Using a renormalization method, we extend the scaling results of intermittency for the 1D map to two coupled 1D maps.

Consider a map T consisting of two identical 1D maps coupled symmetrically,

$$T : \begin{cases} x_{n+1} = f(x_n) + g(x_n, y_n), \\ y_{n+1} = f(y_n) + g(y_n, x_n), \end{cases} \quad (1)$$

where the subscript n denotes a discrete time, $f(x)$ is a 1D map with a quadratic maximum, and $g(x, y)$ is a coupling function obeying a condition,

$$g(x, x) = 0 \text{ for any } x. \quad (2)$$

The two-coupled 1D map (1) is called a symmetric map because it has an exchange symmetry such that

$$\sigma^{-1}T\sigma(\mathbf{z}) = T(\mathbf{z}) \text{ for all } \mathbf{z}, \quad (3)$$

where $\mathbf{z} = (x, y)$, σ is an exchange operator acting on \mathbf{z} such that $\sigma\mathbf{z} = (y, x)$, and σ^{-1} is its inverse. The set of all fixed points of σ forms a synchronization line $y = x$ in the state space. It follows from Eq. (3) that the exchange operator σ commutes with the symmetric map T , i.e., $\sigma T = T\sigma$. Thus the synchronization line becomes invariant under T . An orbit is called a(n) (in-phase) synchronous orbit if it lies on the invariant synchronization line, i.e., it satisfies

$$x_n = y_n \text{ for all } n. \quad (4)$$

Otherwise, it is called an (out-of-phase) asynchronous orbit.

Let us introduce new coordinates X and Y ,

$$X = \frac{x + y}{2}, \quad Y = \frac{x - y}{2}. \quad (5)$$

Then the map (1) becomes

$$\begin{aligned}
X_{n+1} &= F(X_n, Y_n) \\
&= \frac{1}{2} [f(X_n + Y_n) + f(X_n - Y_n)] \\
&\quad + \frac{1}{2} [g(X_n + Y_n, X_n - Y_n) + g(X_n - Y_n, X_n + Y_n)], \\
Y_{n+1} &= G(X_n, Y_n) \\
&= \frac{1}{2} [f(X_n + Y_n) - f(X_n - Y_n)] \\
&\quad + \frac{1}{2} [g(X_n + Y_n, X_n - Y_n) - g(X_n - Y_n, X_n + Y_n)].
\end{aligned} \tag{6}$$

This map is invariant under the reflection $Y \rightarrow -Y$, and hence the invariant synchronization line becomes $Y = 0$. Then the synchronous orbit of the old map (1) becomes the orbit of this new map with $Y = 0$. Furthermore, the X -coordinate of the synchronous orbit satisfies the uncoupled 1D map, i.e., $X_{n+1} = f(X_n)$, because the coupling function g obeys the condition (2).

Stability of a synchronous orbit of period p is determined from the Jacobian matrix M of T^p , which is given by the p product of the linearized map DT of the map (6) along the orbit

$$\begin{aligned}
M &= \prod_{n=1}^p DT(X_n, 0) \\
&= \prod_{n=1}^p \begin{pmatrix} f'(X_n) & 0 \\ 0 & f'(X_n) - 2G(X_n) \end{pmatrix},
\end{aligned} \tag{7}$$

where $f'(X) = df(X)/dX$ and $G(X) = \partial g(X, Y)/\partial Y|_{Y=X}$. The eigenvalues of M , called the Floquet (stability) multipliers of the orbit, are

$$\lambda_1 = \prod_n^p f'(X_n), \quad \lambda_2 = \prod_n^p [f'(X_n) - 2G(X_n)]. \tag{8}$$

Note that λ_1 is just the Floquet multiplier for the case of the uncoupled 1D map and the coupling affects only λ_2 .

Consider a synchronous saddle-node bifurcation to a synchronous periodic orbit. The synchronous periodic orbit is stable when both Floquet multipliers lie inside the unit circle, i.e., $|\lambda_j| < 1$ for $j = 1$ and 2 . Thus its stable region in the parameter plane is bounded by four bifurcation lines, i.e., those curves determined by the equations $\lambda_j = \pm 1$ ($j = 1, 2$). When a Floquet multiplier λ_j increases through 1 , the stable synchronous periodic orbit loses its stability via saddle-node or pitchfork bifurcation. On the other hand, when a Floquet multiplier λ_j decreases through -1 , it becomes unstable via period-doubling bifurcation. (For more details on bifurcations, refer to Ref. [13].)

Here we are interested in intermittency just preceding the synchronous saddle-node bifurcation. Employing an approximate renormalization operator [9,14–16] which includes a truncation, we generalize the 1D scaling results for intermittency to the case of two coupled

1D maps. We thus find two fixed maps of the approximate renormalization operator. They have a common relevant eigenvalue associated with the scaling of the control parameter of the uncoupled 1D map. However, the relevant ‘‘coupling eigenvalue’’ associated with coupling perturbation varies depending on the fixed maps.

Truncating the map (6) at its quadratic terms, we have

$$T_{\mathbf{P}} : \begin{cases} X_{n+1} = A + BX_n + CX_n^2 + FY_n^2 \\ Y_{n+1} = DY_n + EX_nY_n \end{cases}, \quad (9)$$

which is a six-parameter family of coupled maps. Other terms do not appear because $F(X, Y)$ and $G(X, Y)$ in Eq. (6) are even and odd in Y , respectively. Here \mathbf{P} represents the six parameters, i.e., $\mathbf{P} = (A, B, C, D, E, F)$. The construction of Eq. (9) corresponds to a truncation of the infinite dimensional space of coupled maps to a six-dimensional space. The parameters A , B , C , D , E , and F can be regarded as the coordinates of the truncated space.

We look for fixed points of the renormalization operator \mathcal{R} in the truncated six-dimensional space of coupled maps,

$$\mathcal{R}(T) = \Lambda T^2 \Lambda^{-1}. \quad (10)$$

Here the rescaling operator Λ is given by

$$\Lambda = \begin{pmatrix} \alpha & 0 \\ 0 & \alpha \end{pmatrix}, \quad (11)$$

where α is a rescaling factor.

The operation \mathcal{R} in the truncated space can be represented by a transformation of parameters, i.e., a map from $\mathbf{P} \equiv (A, B, C, D, E, F)$ to $\mathbf{P}' \equiv (A', B', C', D', E', F')$,

$$A' = \alpha A(1 + B + AC), \quad (12a)$$

$$B' = B(B + 2AC), \quad (12b)$$

$$C' = \frac{C}{\alpha}(B + B^2 + 2AC), \quad (12c)$$

$$D' = D(D + AE), \quad (12d)$$

$$E' = \frac{E}{\alpha}(BD + D + AE), \quad (12e)$$

$$F' = \frac{F}{\alpha}(2AC + B + D^2). \quad (12f)$$

The fixed point $\mathbf{P}^* = (A^*, B^*, C^*, D^*, E^*, F^*)$ of this map can be determined by solving $\mathbf{P}' = \mathbf{P}$. We thus find two solutions associated with a saddle-node bifurcation, as will be seen below. The map (9) with a solution \mathbf{P}^* ($T_{\mathbf{P}^*}$) is the fixed map of the renormalization transformation \mathcal{R} ; for brevity $T_{\mathbf{P}^*}$ will be denoted as T^* .

For a saddle-node bifurcation at $x = 0$, the 1D map $f(x)$ satisfies

$$f(0) = 0, \quad f'(0) = 1. \quad (13)$$

Hence the function $F(X, Y)$ in Eq. (6) obeys

$$F(0,0) = 0, \quad \left. \frac{\partial F}{\partial X} \right|_{(0,0)} = 1. \quad (14)$$

We first note that Eqs. (12a)-(12c) are only for A , B , C , and α . We find one solution for A^* , B^* , C^* , and α satisfying the conditions (14),

$$\alpha = 2, \quad A^* = 0, \quad B^* = 1, \quad C^* : \text{arbitrary number}. \quad (15)$$

Substituting the values of A^* , B^* and α into Eqs. (12d)-(12f), we have two solutions for D^* , E^* , and F^* ,

$$D^* = 0, \quad E^* = 0, \quad F^* = 0, \quad (16a)$$

$$D^* = 1, \quad E^* : \text{arbitrary number}, \quad F^* : \text{arbitrary number}. \quad (16b)$$

These two solutions are associated with intermittency in the coupled 1D maps, as will be seen below. Hereafter we will call each map from the top as the I and E map, respectively, as listed in Table I.

Consider an infinitesimal perturbation $\epsilon \delta \mathbf{P}$ to a fixed point \mathbf{P}^* of the transformation of parameters (12a)-(12f). Linearizing the transformation at \mathbf{P}^* , we obtain the equation for the evolution of $\delta \mathbf{P}$,

$$\delta \mathbf{P}' = J \delta \mathbf{P}, \quad (17)$$

where J is the Jacobian matrix of the transformation at \mathbf{P}^* .

Since the 6×6 Jacobian matrix J decomposes into smaller blocks, one can easily obtain its eigenvalues. Two of them are

$$\lambda_1 = \left. \frac{\partial C'}{\partial C} \right|_{\mathbf{P}^*} = 1, \quad \lambda_2 = \left. \frac{\partial F'}{\partial F} \right|_{\mathbf{P}^*} = \frac{1 + D^{*2}}{2}. \quad (18)$$

Here λ_1 is an eigenvalue associated with scale change in X , and hence C^* is arbitrary. The eigenvalue λ_2 is also associated with scale change in Y in the case $D^* = 1$; this case corresponds to the E map. Thus F^* for this case becomes arbitrary. However, in the case $D^* = 0$ corresponding to the I map, λ_2 becomes an irrelevant eigenvalue. Note that the I map is invariant under a scale change in Y because $F^* = 0$.

The remaining four eigenvalues are those of the following 2×2 blocks,

$$M_1 = \left. \frac{\partial(A', B')}{\partial(A, B)} \right|_{\mathbf{P}^*} = \begin{pmatrix} 4 & 0 \\ 2C^* & 2 \end{pmatrix}, \quad (19)$$

$$M_2 = \left. \frac{\partial(D', E')}{\partial(D, E)} \right|_{\mathbf{P}^*} = \begin{pmatrix} 2D^* & 0 \\ E^* & D^* \end{pmatrix}. \quad (20)$$

The two eigenvalues of M_i ($i = 1, 2$) are called δ_i and δ'_i , and they are listed in Table II.

The two I and E maps have common eigenvalues of M_1 . They are $\delta_1 = 4$ and $\delta'_1 = 2$, which are just the relevant eigenvalues [3] for the case of uncoupled 1D maps. Here the largest relevant eigenvalue δ_1 is associated with scaling of the control parameter of the 1D map near the intermittency threshold.

The eigenvalues δ_2 and δ'_2 of M_2 are associated with coupling perturbations. These eigenvalues will be referred to as ‘‘coupling eigenvalues’’ (CE’s). The submatrix M_2 for the I map becomes a null matrix, and hence there exist no CE’s. On the other hand, the E map has a relevant CE $\delta_2 = 2$ and a marginal CE $\delta'_2 = 1$. Here the relevant CE δ_2 is associated with scaling of the coupling parameter, while the marginal one δ'_2 is associated with the arbitrary constant E^* .

We also obtain the Floquet multipliers λ_1^* and λ_2^* of the fixed point $(0, 0)$ of the fixed map T^* of the renormalization transformation \mathcal{R} . They are given by

$$\lambda_1^* = 1, \quad \lambda_2^* = D^*. \quad (21)$$

The I and E maps have a common Floquet multiplier λ_1^* , which is just that for the 1D case. However, the second Floquet multiplier λ_2^* affected by coupling depends on the fixed maps; $\lambda_2^* = 0$ (1) for the I (E) map.

In order to confirm the above renormalization results, we also study the intermittency for the linearly-coupled case. The critical set (set of critical points) for the intermittency consists of critical line segments. It is found that the I map with no relevant CE’s governs the critical behavior at interior points of each critical line segment, while the E map with one relevant CE δ_2 ($= 2$) governs the critical behavior at both ends.

We choose $f(x) = 1 - ax^2$ as the uncoupled 1D map in Eq. (1) and consider a linear coupling case $g(x, y) = c(y - x)$. Here c is a coupling parameter. Three critical line segments are found on a synchronous saddle-node bifurcation line $a = a_c$ ($= 1.75$, above which a pair of synchronous orbits with period 3 appears. The critical behaviors near the three critical line segment are the same.

As an example, consider a critical line segment including the zero-coupling point $c = 0$ as one end point. Figure 1 shows a phase diagram near this critical line segment denoted by a solid line. This diagram is obtained from the calculation of two Lyapunov exponents. In case of a synchronous orbit, its Lyapunov exponents are given by

$$\sigma_{\parallel}(a) = \lim_{m \rightarrow \infty} \frac{1}{m} \sum_{n=0}^{m-1} \ln |f'(x_n)|, \quad \sigma_{\perp}(a, c) = \lim_{m \rightarrow \infty} \frac{1}{m} \sum_{n=0}^{m-1} \ln |f'(x_n) - 2c|. \quad (22)$$

Here σ_{\parallel} (σ_{\perp}) denotes the mean exponential rate of divergence of nearby orbits along (across) the synchronization line $y = x$. Hereafter, σ_{\parallel} and σ_{\perp} will be referred to as tangential and transversal Lyapunov exponents, respectively. Note also that σ_{\parallel} is just the Lyapunov exponent for the 1D case, and the coupling affects only σ_{\perp} .

The data points on the $\sigma_{\perp} = 0$ curve are denoted by solid circles in Fig. 1. A synchronous orbit on the synchronization line $y = x$ becomes a synchronous attractor with $\sigma_{\perp} < 0$ inside the $\sigma_{\perp} = 0$ curve. The type of this synchronization attractor is determined according to the sign of σ_{\parallel} . A synchronous period-3 orbit with $\sigma_{\parallel} < 0$ becomes a synchronous periodic attractor above the critical line segment, while there exists a synchronous chaotic attractor with $\sigma_{\parallel} > 0$ below the critical line segment. These periodic and chaotic regions are denoted by P and C in the diagram, respectively. There exists a synchronous period-3 attractor with $\sigma_{\parallel} = 0$ on the critical line segment between these two regions.

The motion on the synchronous chaotic attractor in the region C just below the critical line segment is characterized by the occurrence of intermittent alternations between regular

behavior and chaotic behavior on the synchronization line. This is just the intermittency occurring in the uncoupled 1D map, because the motion on the synchronization line is the same as that for the uncoupled 1D case. Thus, a transition from a regular behavior to an intermittent chaotic behavior, which is essentially the same as that for the 1D case, occurs near the critical line segment joining two end points $c_l = -0.109045\dots$ and $c_r = 0$ on the synchronous saddle-node bifurcation line $a = a_c (= 1.75)$.

Consider a “1D-like” intermittent transition to chaos near an interior point with $c_l < c < c_r$ of the critical line segment. We fix the value of c at some interior point and vary the control parameter ϵ ($\equiv a_c - a$). For $\epsilon < 0$, there exists a synchronous period-3 attractor on the synchronization line. However, as ϵ is increased from zero, an intermittent synchronous chaotic attractor appears. Like the 1D case [3], the scaling relations of the mean duration \bar{l} of regular behavior and the tangential Lyapunov exponent σ_{\parallel} for an intermittent chaotic orbit on the synchronization line are obtained from the leading relevant eigenvalue δ_1 ($= 4$) of the I map, as will be seen below.

We first note that the I map is essentially a 1D map with zero Jacobian determinant (see Table I). Since there exists no relevant CE’s associated with coupling perturbation, it has only relevant eigenvalues δ_1 and δ'_1 like the 1D case. The I map is therefore associated with the critical behavior at interior points of the critical line segments.

A map with non-zero ϵ near a critical interior point is transformed to a new map of the same form, but with a new parameter ϵ' under a renormalization transformation \mathcal{R} . Here the control parameter scales as

$$\epsilon' = \delta_1 \epsilon = 2^2 \epsilon. \quad (23)$$

Then the mean duration \bar{l} and the tangential Lyapunov exponent σ_{\parallel} satisfy the homogeneity relations,

$$\bar{l}(\epsilon') = \frac{1}{2} \bar{l}(\epsilon), \quad \sigma_{\parallel}(\epsilon') = 2 \sigma_{\parallel}(\epsilon), \quad (24)$$

which lead to the scaling relations,

$$\bar{l}(\epsilon) \sim \epsilon^{-\mu}, \quad \sigma_{\parallel}(\epsilon) \sim \epsilon^{\mu}, \quad (25)$$

with exponent

$$\mu = \log 2 / \log \delta_1 = 0.5. \quad (26)$$

The above 1D-like intermittent transition to chaos ends at both ends of the critical line segment. We fix the value of the control parameter $a = a_c$ ($= 1.75$) and study the critical behavior near both ends c_l and c_r by varying the coupling parameter c . Inside the critical line segment ($c_l < c < c_r$), a synchronous period-3 attractor with $\sigma_{\perp} < 0$ exists on the synchronization line, and hence the coupling tends to synchronize the interacting systems. However, as the coupling parameter c passes through both ends, the transversal Lyapunov exponent σ_{\perp} of the synchronous periodic orbit grows continuously from zero, and hence the coupling leads to desynchronization of the interacting systems. The synchronous orbit of period 3 is therefore no longer an attractor outside the critical line segments, and a new asynchronous attractor appears.

The critical behaviors near both ends are the same. As an example, consider the case of the zero-coupling point $c_r = 0$. Figure 2 shows the plot of σ_\perp versus c for $a = a_c$. Note that σ_\perp increases linearly with respect to c . Hence a transition from a synchronous to an asynchronous state occurs at the zero-coupling end point.

The scaling relation of $\sigma_\perp(c)$ for $a = a_c$ is obtained from the relevant CE δ_2 ($= 2$) of the E map as follows. Consider a map with non-zero c near the zero-coupling point. It is then transformed to a map of the same form, but with a renormalized parameter c' under a renormalization transformation \mathcal{R} . Here the coupling parameter obeys a scaling law,

$$c' = \delta_2 c = 2c. \quad (27)$$

Then the transversal Lyapunov exponent σ_\perp satisfies the homogeneity relation,

$$\sigma_\perp(c') = 2\sigma_\perp(c). \quad (28)$$

This leads to the scaling relation,

$$\sigma_\perp(c) \sim c^\nu, \quad (29)$$

with exponent

$$\nu = \log 2 / \log \delta_2 = 1. \quad (30)$$

Like the case of the I map, the scaling behavior of $\sigma_\parallel(\epsilon)$ for $c = c_l$ or c_r is obtained from the relevant eigenvalue δ_1 ($= 4$) of the E map, and hence it also satisfies the scaling relation (25). The critical behaviors of both exponents σ_\parallel and σ_\perp near an end point are thus determined from two relevant eigenvalues δ_1 and δ_2 of the E map. An extended version of this work including the results of a renormalization analysis without truncation, the results for the many-coupled cases and so on will be given elsewhere [17]

ACKNOWLEDGMENTS

This work was supported by the the Korea Research Foundation under Project No. 1997-001-D00099.

REFERENCES

- [1] P. Manneville and Y. Pomeau, Phys. Lett. A **75**, 1 (1979); Physica D **1**, 219 (1980); Y. Pomeau and P. Manneville, Commun. Math. Phys. **74**, 189 (1980).
- [2] J-P Eckmann, L. Thomas and P. Wittwer, J. Phys. A **14**, 3153 (1981); J. E. Hirsh, B. A. Hubermann and D. J. Scalapino, Phys. Rev. A **25**, 519 (1982).
- [3] J. E. Hirsh, M. Nauenberg, and D. J. Scalapino, Phys. Lett. A **87**, 391 (1982); B. Hu and J. Rudnick, Phys. Rev. Lett. **48**, 1645 (1982).
- [4] M. J. Feigenbaum, J. Stat. Phys. **19**, 25 (1978); **21**, 669 (1979).
- [5] I. Waller and R. Kapral, Phys. Rev. A **30**, 2047 (1984); R. Kapral, Phys. Rev. A **31**, 3868 (1985).
- [6] S. P. Kuznetsov, Radiophys. Quantum Electron. **28**, 681 (1985); S. P. Kuznetsov and A. S. Pikovsky, Physica D **19**, 384 (1986); H. Kook, F. H. Ling, and G. Schmidt, Phys. Rev. A **43**, 2700 (1991).
- [7] I. S. Aranson, A. V. Gaponov-Grekhov and M. I. Rabinovich, Physica D **33**, 1 (1988).
- [8] S.-Y. Kim and H. Kook, Phys. Rev. A **46**, R4467 (1992); Phys. Rev. E **48**, 785 (1993); S.-Y. Kim, Phys. Rev. E **49**, 1745 (1994).
- [9] S.-Y. Kim and H. Kook, Phys. Lett. A **178**, 258 (1993)
- [10] K. Kaneko, in *Theory and applications of coupled map lattices*, edited by K. Kaneko (John Wiley & Sons, New York, 1992), p. 1, and references cited therein.
- [11] S.-Y. Kim and K. Lee, Phys. Rev. E **54**, 1237 (1996).
- [12] S.-Y. Kim, Phys. Rev. E **52**, 1206 (1995); Phys. Rev. E **54**, 3393 (1996).
- [13] J. Guckenheimer and P. Holmes, *Nonlinear Oscillations, Dynamical Systems, and Bifurcations of Vector Fields* (Springer-Verlag, New York, 1983), Sec. 3.5.
- [14] J. Greene, R. S. MacKay, F. Vivaldi and M. J. Feigenbaum, Physica D **3**, 468 (1981).
- [15] J.-M. Mao and J. Greene, Phys. Rev. A **35**, 3911 (1987).
- [16] A. Lahiri, Phys. Rev. A **45**, 757 (1992).
- [17] S.-Y. Kim (unpublished).

TABLES

TABLE I. Fixed point \mathbf{P}^* of the renormalization transformation \mathcal{R} and the rescaling factor α .

| fixed map | α | A^* | B^* | C^* | D^* | E^* | F^* |
|-----------|----------|-------|-------|-----------|-------|-----------|-----------|
| I map | 2 | 0 | 1 | arbitrary | 0 | 0 | 0 |
| E map | 2 | 0 | 1 | arbitrary | 1 | arbitrary | arbitrary |

TABLE II. Some eigenvalues $\delta_1, \delta'_1, \delta_2,$ and δ'_2 of a fixed map T^* of the renormalization operator are shown.

| fixed map | δ_1 | δ'_1 | δ_2 | δ'_2 |
|-----------|------------|-------------|-------------|-------------|
| I map | 4 | 2 | nonexistent | nonexistent |
| E map | 4 | 2 | 2 | 1 |

FIGURES

FIG. 1. Phase diagram of the two-coupled 1D map (1) with $f(x) = 1 - ax^2$ and $g(x, y) = c(y - x)$. Here solid circles denote the data points on the $\sigma_{\perp} = 0$ curve. The region enclosed by the $\sigma_{\perp} = 0$ curve is divided into two parts denoted by P and C. A synchronous period-3 (chaotic) attractor with $\sigma_{\parallel} < 0$ ($\sigma_{\parallel} > 0$) exists in the subregion P (C). The boundary curve denoted by a solid line between the P and C regions is just a critical line segment.

FIG. 2. Plot of the transversal Lyapunov exponent σ_{\perp} of a synchronous period-3 orbit versus c for $a = a_c$ ($= 1.75$).

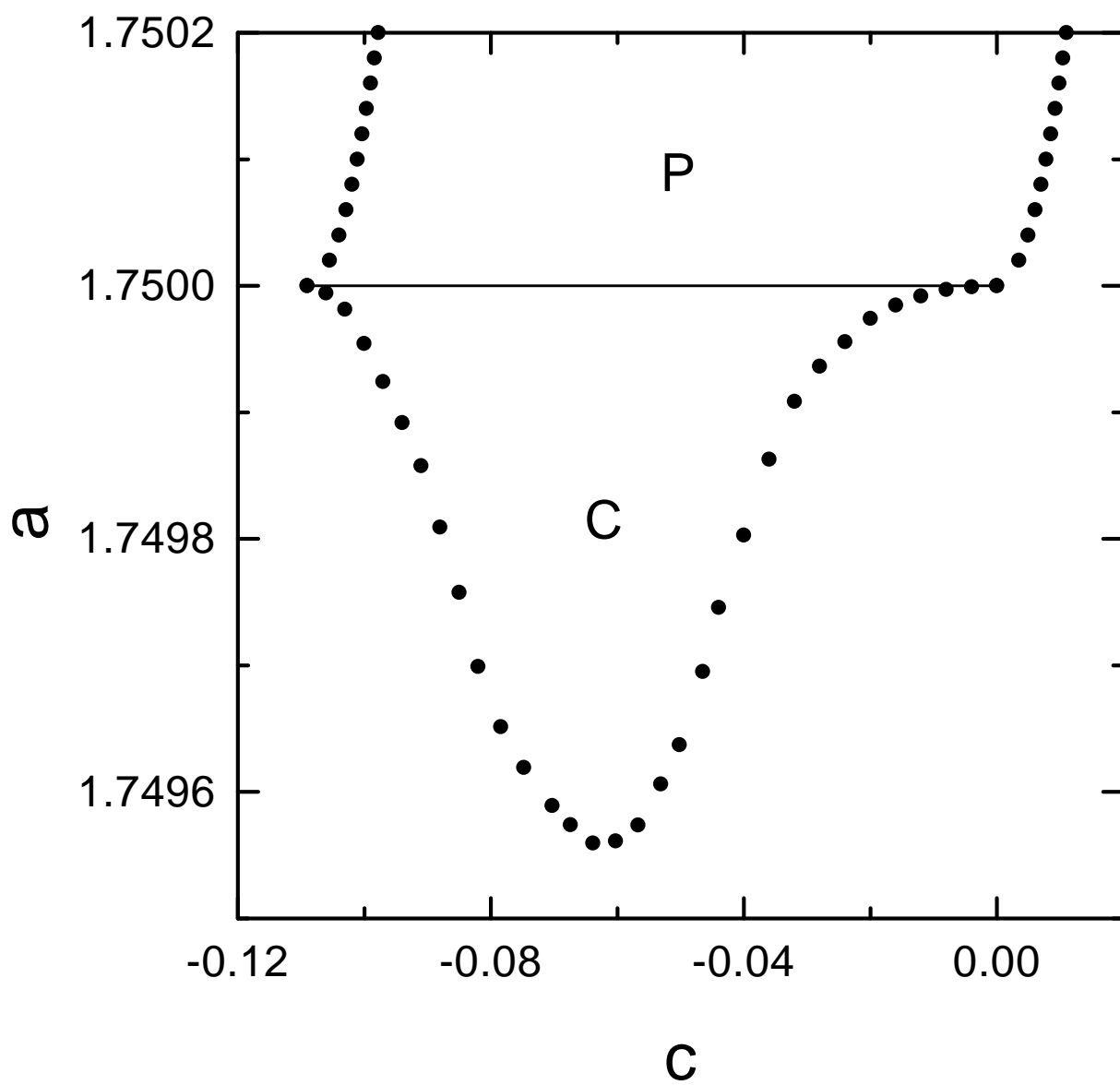


Fig. 1 (Kim,PL-A)

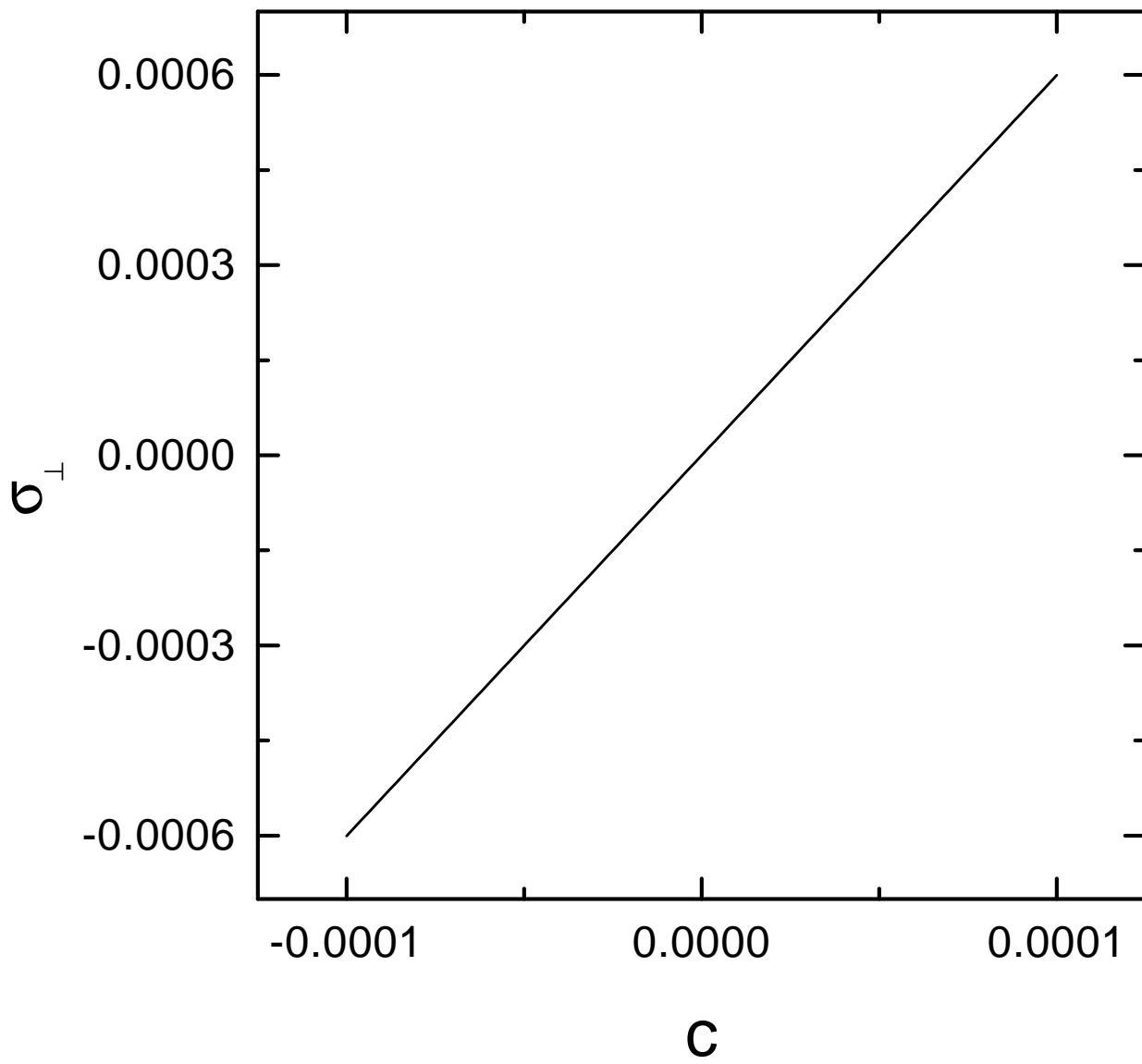


Fig. 2 (Kim,PL-A)